KAUNAS UNIVERSITY OF TECHNOLOGY
VYTAUTAS MAGNUS UNIVERSITY

ARŪNAS KLEIVA

RESEARCH AND DEVELOPMENT OF VIBRATION ENERGY HARVESTER FOR WEARABLE BIOMECHATRONIC SYSTEMS

Summary of Doctoral Dissertation
Technological Sciences, Mechanical Engineering (T 009)

2019, Kaunas

This doctoral dissertation was prepared at Kaunas University of Technology, Faculty of Mechanical Engineering and Design, Institute of Mechatronics during the period of 2014–2018.

Scientific Supervisor:
Dr. Rolanas DAUKŠEVIČIUS (Kaunas University of Technology, Technological Sciences, Mechanical Engineering, T 009).

Editor: Dovilė Dumbrauskaitė (Publishing Office "Technologija")

Dissertation Defence Board of Mechanical Engineering Science Field:
Prof. Dr. Habil. Vytautas OSTAŠEVIČIUS (Kaunas University of Technology, Technological Sciences, Mechanical Engineering, T 009) – **chairman**;
Prof. Dr. Dalius MAŽEIKA (Vilnius Gediminas Technical University, Technological Sciences, Mechanical Engineering, T 009);
Assoc. Prof. Dr. Giedrius JANUŠAS (Kaunas University of Technology, Technological Sciences, Mechanical Engineering, T 009);
Dr. János VOLK (Hungarian Academy of Sciences, Institute of Technical Physics and Materials Science, Material Engineering);
Prof. Dr. Vytautas JŪRĖNAS (Kaunas University of Technology, Technological Sciences, Mechanical Engineering, T 009).

The official defence of the dissertation will be held at 12 noon on 7th of June, 2019 at the public meeting of Dissertation Defence Board of Mechanical Engineering Science Field in Dissertation Defence Hall at Kaunas University of Technology.

Address: K. Donelaičio St. 73-403, 44249 Kaunas, Lithuania.
Tel. no. (+370) 37 300 042; fax. (+370) 37 324 144; e-mail doktorantura@ktu.lt.

Summary of doctoral dissertation was sent on 7th May, 2019.
The doctoral dissertation is available on the internet http://ktu.edu and at the libraries of Kaunas University of Technology (K. Donelaičio St. 20, 44239 Kaunas, Lithuania) and Vytautas Magnus University Agriculture Academy (Studentų St. 11, Akademija, 53361 Kauno raj., Lithuania).

KAUNO TECHNOLOGIJOS UNIVERSITETAS
VYTAUTO DIDŽIOJO UNIVERSITETAS

ARŪNAS KLEIVA

DĖVIMŲ BIOMECHATRONINIŲ SISTEMŲ VIBRACINIO ELEKTROS ENERGIJOS ŠALTINIO KŪRIMAS IR TYRIMAS

Daktaro disertacijos santrauka
Technologijos mokslai, mechanikos inžinerija (T 009)

2019, Kaunas

Disertacija rengta 2014-2018 metais Kauno technologijos universiteto Mechanikos inžinerijos ir dizaino fakultete Mechatronikos institute.

Mokslinis vadovas:
Dr. Rolanas DAUKŠEVIČIUS (Kauno technologijos universitetas, Technologijos mokslai, mechanikos inžinerija, T 009).

Redagavo: Dovilė Dumbrauskaitė (Leidykla "Technologija")

Mechanikos inžinerijos mokslo krypties disertacijos gynimo taryba:
Prof. habil. dr. Vytautas OSTAŠEVIČIUS (Kauno technologijos universitetas, Technologijos mokslai, mechanikos inžinerija, T 009) – **pirmininkas**;
Prof. dr. Dalius MAŽEIKA (Vilniaus Gedimino technikos universitetas, Technologijos mokslai, mechanikos inžinerija, T 009);
Doc. dr. Giedrius JANUŠAS (Kauno technologijos universitetas, Technologijos mokslai, mechanikos inžinerija, T 009);
Dr. János VOLK (Vengrijos mokslų akademija, Technologijos mokslai, medžiagų inžinerija, T 008);
Prof. dr. Vytautas JŪRĖNAS (Kauno technologijos universitetas, Technologijos mokslai, mechanikos inžinerija, T 009).

Disertacija bus ginama viešame mechanikos inžinerijos mokslo krypties disertacijos gynimo tarybos posėdyje 2019 m. birželio 7 d. 12 val. Kauno technologijos universiteto disertacijų gynimo salėje.

Adresas: K. Donelaičio g. 73-403, 44249 Kaunas, Lietuva.
Tel. (370) 37 300 042; faks. (370) 37 324 144; el. paštas doktorantura@ktu.lt.

Disertacijos santrauka išsiųsta 2019 m. gegužės 7 d.
Su disertacija galima susipažinti internetinėje svetainėje http://ktu.edu ir Kauno technologijos universiteto bibliotekoje (K. Donelaičio g. 20, 44239 Kaunas) ir Vytauto didžiojo universiteto žemės ūkio akademijos bibliotekoje (Studentų g. 11, Akademija, 53361 Kauno raj.).

INTRODUCTION

Research relevance, aim and objectives

During the last several decades the progress in microfabrication techniques and ultra-low power integrated circuits has encouraged the development of various portable, wearable and implantable smart devices for a wide range of wireless communication, fitness tracking, navigation, physiological sensing, etc. Unfortunately, conventional batteries now used in such devices have insufficient energy density, which leads to a necessity of regularly recharging or replacing them. The disposal of electrochemical energy modules is related to environmental hazards. As a consequence, micro energy harvesting was developed as a separate actively growing research field in order to reduce the heavy need of battery technology which obstructs higher advancements in wearable electronics. The past 10–15 years have shown an increase in research activities on alternative biomechanical energy harvesting since a large amount of human-based mechanical energy could be converted to electrical energy. A promising energy conversion method is vibrational piezoelectric energy harvesters (V-PEHs) with inserted smart materials. For example, V-PEHs are highly suitable for autonomous, self-charging smart devices because of their high energy density and possible implementation at macro/micro/nano scales.

The aim of this research is to design, fabricate and experimentally analyze a biomechanical piezoelectric energy harvester (PEH) for useful micro-power generation under ultra-low frequency random human body excitations. In order to achieve the aim, the following objectives are raised:

1. To review literature considering the existing vibration energy harvesters by focusing on piezo-generators that employ mechanical frequency up-conversion.
2. To implement numerical models of magnetic interaction, perform analytical and experimental verification and evaluate the dynamic characteristics of magnetic force impulses.
3. To perform a systematic numerical-experimental study of magnetic frequency up-converting piezo-generator and determine the main dynamic principles and quantitative criteria needed to design effective piezo-generators.
4. To implement and verify a dynamic numerical model of the magnetic frequency up-converting piezo-generator and calculate its vibrational and electrical responses.

5. To propose and analyze methods for increasing the effectiveness of magnetic frequency up-conversion and improving micro-power generation under low-frequency biomechanical excitations.
6. To design a wearable piezoelectric biomechanical energy harvester that integrates the proposed methods for increasing the effectiveness, fabricate a semi-printed proof-of-concept harvester and test it under realistic operational conditions.

Research methods

This research work was accomplished using theoretical and experimental study methods. The theoretical study was developed by using analytical and numerical methods. SolidWorks, COMSOL Multiphysics and Microsoft Excel with Visual Basic were used for designing, finite element modeling and data processing. The experimental research was performed at the Institute of Mechatronics using Polytec Doppler vibrometer (LDV), Magnet-Physik Teslameter, Wayne Kerr impedance analysis systems, the realistic operation conditions were tested with Zebris Rehawalk® treadmill. Various parts of proof-of-concept device were made using EOS Formiga and Ultimaker 3D prototyping equipment.

Scientific novelty

1. The main dynamic principles and dimensionless excitation parameters that govern the operation of the magnetic frequency up-converting piezo-generators and allow to maximize vibration energy harvesting performance.
2. Computationally efficient magneto-dynamic and magneto-piezo-mechanical finite element models, which together with the identified governing dynamic criteria enable a rational design of the frequency up-converting piezo-generators of arbitrary natural frequency and magnetic configuration that generate maximized power output.
3. Two methods for improving operational effectiveness, which exploit magnet speed amplification and synchronized multi-magnet excitation, enabling near-silent and reliable operation of frequency up-converting piezo-generators in the maximized power regime (around transient resonance) for various biomechanical excitation conditions.

Defended statements

1. Frequency up-converting piezo-generator delivers maximized power when impulsive magnetic excitation induces transient resonance, when the vibration

frequency of the transducer becomes close to the natural frequency in all stages of the response.
2. The multiphysics magneto-piezo-mechanical finite element model is computationally efficient and allows to predict the dynamic and electric characteristics of the piezo-generators with acceptable accuracy.
3. The magnet speed amplification method is an effective and robust excitation approach which ensures the operation of the piezo-generator in the maximized power regime (around transient resonance) when excited by active movement of human arms.
4. The synchronized multi-magnet excitation method is effective and ensures an about 30% increase in power output per single operational cycle when using two driving magnets (in comparison to the single-magnet excitation case).
5. The proof-of-concept piezo-generator has an original design which rationally integrates magnetic amplification and multi-magnet excitation subsystems, ensuring nearly silent operation in the maximized power regime under varying jogging speeds.

Practical value

1. The implemented finite element models and the identified governing dynamic criteria are useful for the rational design of magnetic frequency up-converting piezo-generators of arbitrary design.
2. The implemented multi-channel non-contact measurement setup registers dynamic, electric and magnetic signals and is suitable for detailed experimental study of piezo-generators of different magnetic configuration.
3. The proposed methods of magnetic amplification and multi-magnet excitation may be adapted for increasing the effectiveness of various magnetic frequency up-converting piezo-generators.
4. The demonstrated proof-of-concept piezo-generator may be miniaturized and adapted for recharging batteries of various portable or wearable electronics (fitness trackers, smart devices, etc.).

Research approbation

The results of this dissertation were published in 5 scientific papers: 2 – in journals with impact factor indexed in Web of Science database, 3 – in conference proceedings.

The research results were also presented at 3 international scientific conferences: Mechanika 2015 (Kaunas, Lithuania), Mechanika 2016 (Kaunas, Lithuania) and EuroSimE 2019 (Hannover, Germany).

Structure of the dissertation

The dissertation consists of an introduction, nomenclature, four chapters, general conclusions, a list of references and scientific publications on the topic of dissertation.

The volume of the dissertation is 109 pages, 46 figures and 5 tables. The list of references consists of 132 sources.

1. LITERATURE REVIEW

During the last several decades the progress in microfabrication techniques and ultra-low power integrated circuits has encouraged the development of various portable, wearable and implantable smart devices for a wide range of wireless communication, fitness tracking, navigation, physiological sensing, etc. technologies [1, 3]. Unfortunately, conventional batteries now used in such devices have insufficient energy density, which leads to the necessity of regularly recharging or replacing them. The disposal of electrochemical energy modules is related to environmental hazards. Micro energy harvesting was developed as a separate actively growing research field in order to reduce the heavy need of battery technology which obstructs higher advancements in wearable electronics [1]. Recent research has shown that a large amount of human-based biomechanical energy could be converted to electrical energy. Piezoelectric, electrostatic, electromagnetic and triboelectric mechanisms are commonly used for mechanical-to-electrical energy conversion. The piezoelectric energy harvesters (PEHs) considered in this study are highly suitable for autonomous, self-charging smart wearables because of their high energy density and possible implementation at macro/micro/nano scales. Ultra-low frequency (< 1–10 Hz), multi-directional and time-varying human body movements (e.g. limbs) lead to essential challenges in designing efficient and effective PEHs, which are usually based on high stiffness transducers that are configured as underdamped (high-Q) linear oscillators. In this case, high output power is delivered only when the transducer is excited at relatively high resonant frequencies (> 50–100 Hz). The level of output power is proportional to the cube of natural frequency (considering constant displacement amplitude of base excitation) [3,5]. This implies that direct human-induced vibrations are not suitable for efficient energy harvesting application of linear PEHs.

In order to eliminate the aforementioned limitations, mechanical frequency up-conversion (MFU) was developed to boost the operating frequency from the low excitation frequency. Commonly, MFU is based on a two-stage configuration,

where the elastic or rigid driving element affected by external low-frequency excitation impulsively induces high-frequency natural oscillations of a transducer (generating element) by using contact or contactless interaction. Contactless MFU typically relies on fast deflection and release (i.e. plucking) of the transducer by means of magnetic coupling between the moving (driving) magnet(s) and the transducer magnetic end mass(es). For the transducer to operate in optimal operation mode, an effective MFU mechanism has to provide abrupt impulsive (sharp) excitation regardless of the input frequency. Contactless magnetic MFU has more advantages due to the higher robust and is appropriate to noiseless implementations comparing with contact-type plucking, where the transducer has to withstand impact-induced wear and damage with noise issues. Meanwhile the contact-type plucking disadvantages may be reduced by developing a rational design of contacting surfaces; however it could not eliminate physical contact completely [2,4].

2. NUMERICAL STUDY

2.1 Magnetically-excited piezoelectric energy harvester

The configuration of the analyzed magnetically-excited piezoelectric energy harvester (ME-PEH) is presented in figure 1. The system involves a commercially available clamped cantilevered bimorph transducer (PZT-5A made by Piezo Systems with the dimensions of 57.2 mm × 31.8 mm, which has a neodymium cuboidal N52 driven magnet of size 5 × 5 × 3 mm attached at the end. This type of transducer was selected because of its high strain constants, permittivity and high voltage output. The transducer starts to oscillate at high-frequency free vibrations (at natural frequency f_n) when subject to magnetic plucking which is caused when driving magnet transverses near the driven one. Driving magnet motion is achieved by attaching it on a table with the radius of r_T = 80 mm, which spins at rotational speed ω_{rpm}. The relatively large radius of the rotating table imitates a transversion of the driven magnet by the driving one along the linear trajectory in a plucking event. Linear speed, referred to as *plucking speed*, v_{exc} is calculated as follows: $v_{exc} = r_T\omega_{rpm}(2\pi/60)$.

This chapter refers to the presented ME-PEH as *in-plane* plucking arrangement since the transducer deflection and the driving magnet motion directions are in the same plane (*xy* plane). ME-PEH engages direct magnetic configuration by which both magnets are aligned along the *z*-axis without offset in the *z* direction. The essential parameter which defines the distance between the driven and driving magnets along the *x*-axis (when their positions with respect to the *y*-axis are congruent) is *clearance* d_{exc}. The developed plucking configuration may be attractive or repulsive, depending on the pole orientation of the magnets (when both magnets are spatially orientated so that their magnetic axes are parallel to the *x*-axis). Further analysis is based on attractive configuration since the effect of attractive to repulsive configurations (in an ideal case of theoretical model) is analogous except the magnetic force impulses are inverted (with respect to the *x*-axis). Generally, v_{exc} and d_{exc} defines *plucking regime*, MFU conditions and overall vibration energy harvesting performance.

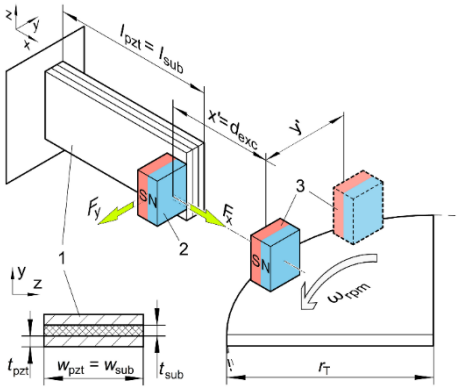

Figure 1. A schematic diagram of the magnetically-excited piezoelectric energy harvester (in-plane arrangement): 1 – bimorph transducer, 2 – magnetic tip mass (driven magnet), 3 – driving magnet.

We assume that a transducer may be constituted as an underdamped second-order dynamic system which is affected by transient magnetic coupling excitation, where magnetic coupling is specified as a complex loading case with several magnetic force components which operate along different axes and generate dissimilar shape impulses. In general, the response of the second-order dynamic system to transient excitation is determined by the relationship between the loading force ramping rate and the system response speed, which depends on the natural frequency f_n and mechanical damping ratio ζ_m. The response speed may be described as the *rise time*, which could be approximated as $t_R \cong 0.5\,\tau_n \cong 0.25T_n$, where T_n and τ_n – natural period and half-period of the transducer, respectively. Magnetic excitation should lead to a sufficiently sharp magnetic plucking action that corresponds to an abrupt deflection and a release of the transducer that induces minimally magnetically impeded free vibrations. Hence, it is necessary to ensure a sufficiently high magnetic force ramping rate.

2.2 Modelling the magnetic interaction

Temporal characteristics of the force impulses produced by the driving and driven magnets may be calculated with analytical and numerical techniques. Magnetic flux density (***B***-field) and magnetic field strength (***H***-field) may be evaluated outside and inside the magnets by using the Amperian and Coulombian modelling approaches, respectively. Usually, a numerical analysis of magnetic interactions is performed by using finite element (FE) method, which is highly convenient and versatile, but may demand high computational resources in specific simulation proposals, e.g. magnetodynamic modelling involves dynamic mesh updating while solving magnetic forces in the air domain. In this study we decided to use the FE method since the developed models could be unconsciously upgraded to simulate other various cases of magnetic plucking in both static and dynamic regimes (e.g. complex shapes and/or different arrangements of the magnets).

Stationary (magnetostatic) and time-dependent (magnetodynamic) simulations of the attractive interaction between two parallel-aligned cuboidal permanent magnets was performed with FE modeling software COMSOL Multiphysics® (figure 2). The magnetostatic model was realized in 3D, while the magnetodynamic one was simplified to 2D in order to reduce the demand of computational cost, thereby ensuring a correct solution convergence and acceptable solution times. The models are based on the AC/DC module with the interface of Magnetic Fields, No Currents. The magnetodynamic model additionally uses the Mathematics module with the Moving Mesh interface (realization of the Arbitrary Lagrange-Eulerian (ALE) method in COMSOL). An analysis of both FE models is made simultaneously since they share essential features.

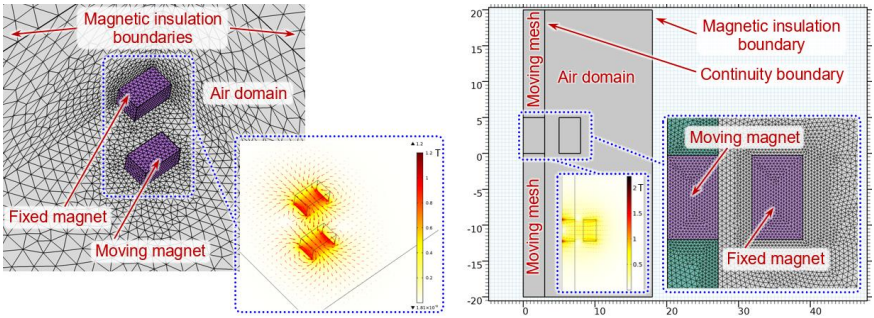

Figure 2. (a) 3D magnetostatic and (b) 2D magnetodynamic FE models of two interacting magnets with a visualization of ***B***-field distribution. The moving and fixed magnets correspond to the driving and driven magnets of ME-PEH, respectively.

2.3 Simulation results

During the in-plane plucking, when the driving magnet traverses near the driven one, the induced transient excitation is caused by the evolution of the axial F_x and transverse F_y magnetic force components (figure 3(a-b)) which determine the properties of the resulting magnetic coupling. F_y is the direct deflection force component, while F_x produces a bending moment onto the transducer. Furthermore, the contribution of M_x and M_y magnetic torques on the dynamic response may be neglected since the transducer is relatively long, i.e. simulations disclose that the influence of M_x and M_y is insignificant, while the contribution of M_z is more than an order of magnitude smaller with respect to the contribution of the forces (e.g. ~20 times smaller in the case of $x' = d_{exc} = 1$ mm). Figure 3(a-b) shows F_x and F_y profiles that are presented as functions of varying transverse displacement y'. Here the evolution of magnetic forces may be described as three distinct stages: ① *activation*, ② *directionality reversal* and ③ *deactivation*. The stage of directionality reversal leads to a jump of amplitude from the maximum positive to the minimum negative point. F_y profile may be described as a symmetrical full-cycle impulse [27], since it consists of two identical half-cycles. Even more, each half-cycle is unsymmetrical due to unequal force ramping rates at the rise and decay sides (figure 4(b)). Meanwhile F_x is a symmetrical half-cycle impulse that may be approximately expressed by a bell-shaped profile function (e.g. half-sine, versed-sine, Gaussian).

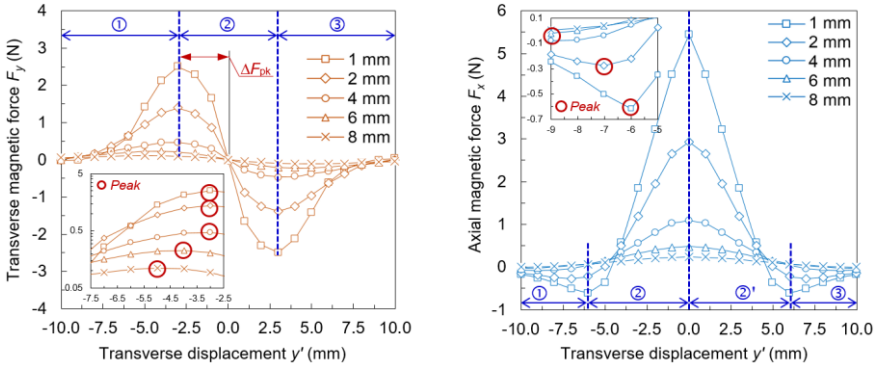

(a) (b)

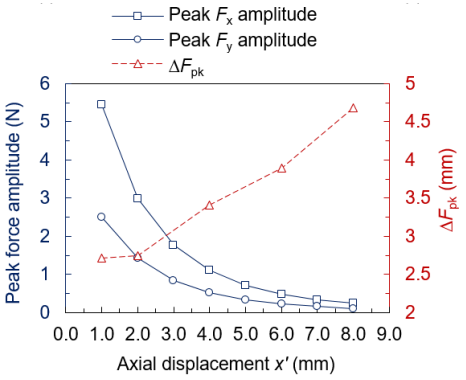

(c)

Figure 3. Simulated static evolution profiles of (a) transverse and (b) axial magnetic force components versus transverse displacement of the driving magnet for $x' = d_{exc}$ = 1–8 mm (insets: semi-log plot illustrating peak shifts with changing x'). Stages of force evolution: ① activation, ②,②' directionality reversal and ③ deactivation.

Generally, the noticeable dissimilarities in force profiles turn into differences in the interaction between the magnetic forces and the restoring forces of the transducer. During in-plane plucking configuration, the process of F_y directionality reversal induces a non-linear jump phenomenon that causes clean free vibrations. We note that energy harvesting performance is determined by the shape parameters of the dominant transducer deflection-inducing force impulse. E.g. the bell-shaped F_x profile could be described by *impulse duration* $t_{MP}(F_x)$ and *ramping time* $t_R(F_x) \cong 0.5\ t_{MP}(F_x)$ (figure 4(a)), which is the duration of primary rise of the axial force to its peak (figure 4(b)). Shorter impulses (ramping time) correspond to the narrower F_x impulse and the higher force ramping rate. The F_y *amplitude jump duration* t_{jump} describes a duration of directionality reversal stage, which has an essential influence on the ME-PEH dynamics during in-plane plucking. Consequently, the ramping time could be defined as $t_R(F_y) = 0.5t_{jump}$.

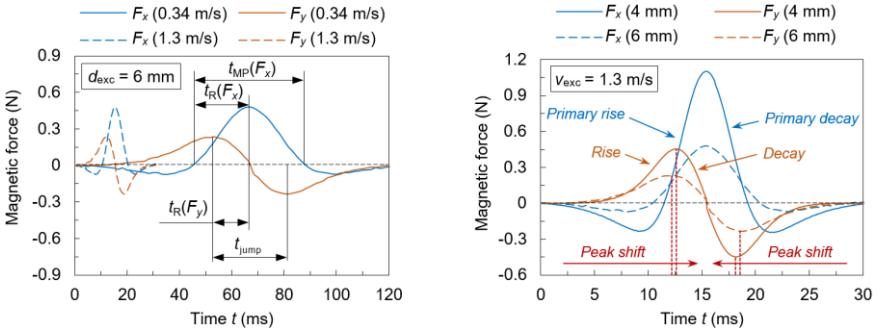

Figure 4. Simulated impulses of transverse and axial magnetic forces for (a) different magnet motion speeds v_{exc} and (b) different clearances d_{exc}.

Numerical simulations were supplemented with experimental data in order to ensure the credibility of the subsequent analysis. We compared the experimental magnetic flux density $t_{ramp}(B_x)$ and simulated magnetic forces $t_{ramp}(F_x) = 0.5t_{MP}(F_x)$ ramping times (Figure 5a). The relevant ramping time of the main plucking caused the force component F_y to be defined as $t_{ramp}(F_y) = 0.5t_{jump}$ (where t_{jump} forces directionality reversal duration). Experimental and measured results show the same trend with a larger v_{exc} by reducing non-linearly with a decreasing rate of change (Figure 5(b)). We note that the measured $t_{ramp}(B_x)$ values are higher by ~10% with respect to the simulated $t_{ramp}(F_x)$ because the magnetometer recorded magnetic flux density B_x and not the real magnetic forces. Also, simulations expressed the real magnetic forces, which act directly on the driven magnet, meanwhile magnetic flux density was measured at the middle of driving and driven magnets.

Simulations reveal that changes in clearance d_{exc} lead to a modification of the properties of F_x and F_y profiles and the interrelation between them. For instance, a reduction in d_{exc} non-linearly increases F_x and F_y peak amplitudes and diminishes the x-axis interval ΔF_{pk} (figure 3(a)) between the peak F_x and F_y amplitude points. More precisely, static F_y profile demonstrates that as d_{exc} is reduced, F_y is (de)activated closer to the neutral position $y' = 0$, which reveals itself as the shifting of F_y peak amplitude point toward $y' = 0$ (i.e. a decrease of ΔF_{pk} in figure 3(a)). In a time-dependent case, this turns into F_y being activated later and deactivated earlier (visible by temporal shifting of the peak amplitude points in figure 4(b)). This means that under a given constant speed v_{exc} it leads to smaller t_{jump} and $t_R(F_y)$. Accordingly, static F_x profile also leads to a shifting of the minimum amplitude points with reduction in d_{exc} (figure 3(b)), where F_x crosses x-axis and turns into the primary rise, which occurs closer to $y' = 0$. In the dynamic case it translates into decreasing $t_{MP}(F_x)$.

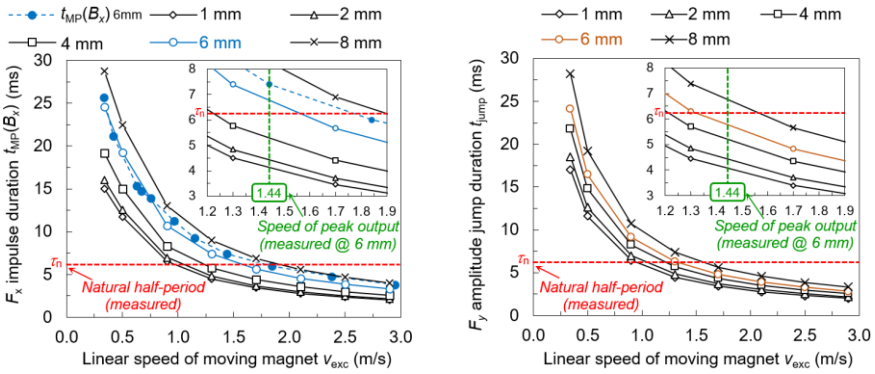

Figure 5. (a) Durations of measured (B_x) and simulated (F_x) excitation impulses versus linear magnet speed for $x' = d_{exc}$ = 1–8 mm. (b) Computed F_y amplitude jump duration versus magnet speed. Insets: close-up of v_{exc} region that encompasses the experimentally determined range of highly effective plucking speeds (~1.44–1.84 m/s) for d_{exc} = 6 mm).

3. EXPERIMENTAL STUDY

3.1 Test setup

In order to test the ME-PEH, dynamic, electric and magnetic transient responses were measured by using a setup that is comprised of three subsystems: magnetic excitation, measurement, and data acquisition (figure 6). During experiments the rotating table speed ω_{rpm} was controlled in the range of 12–350 rpm, which matches the linear (plucking) speed of v_{exc} = 0.10–2.93 m/s. It was monitored using the Polytec rotational laser Doppler vibrometer (LDV) comprised of a sensor head RLV-500 and controller RLV-5000. The driven magnet was tightly attached to the commercially-available transducer (Piezo Systems T226-A4-503Y) tip. In order to precisely adjust magnetic clearance d_{exc}, the transducer was fastened to a micro-positioning stage, where d_{exc} was adjusted in the range of 4–8 mm. Transducer dynamic responses (displacement d_{PT} and velocity v_{PT}) were measured at its tip using the other Polytec LDV with an autofocusing sensor head

Figure 6. A schematic diagram of the experimental setup used for ME-PEH characterization: 1 – transducer (Piezo Systems T226-A4-503Y), 2 – magnetic tip mass (driven magnet), 3 – driving magnet; 4 – rotating table, 5 – micro-positioning stage, 6 – DC motor, 7 – DC power supply (Mastech HY3020E), 8 – LDV sensor head (Polytec OFV-505), 9 – Rotational LDV sensor head (Polytec RLV-500), 10 – LDV controllers (Polytec OFV-5000 and RLV-5000), 11 – 4-channel digital oscilloscope (PICO 6403); 12 – Magnetometer (Magnet-Physik FH-54); 13 – magnetometer sensor (transverse Hall probe HS-TGB5); 14 – adjustable resistance box (IET LABS RS-200-SC); 15 – retroreflective tape.

OFV-505 and controller OFV-5000. Retroreflective tape was placed on the rotating table and the transducer in order to increase the collection of the back-scattered laser light. Magnetic flux density along the x-axis B_x was measured by using a Hall probe magnetometer, which measured the intensity of the magnetic field approximately in the middle of the clearance between the driving and driven magnets.

The data acquisition system contains a 4-channel digital oscilloscope that records voltage signals provided by the transducer, both LDV controllers and the magnetometer. The transducer was connected to the resistance box for adjusting external load resistance R_L. In order to analyze energy harvesting performance under maximized power output conditions all the measurements were made with the ME-PEH connected to the experimentally determined matched load R_{ML}.

3.2 Determination of matched load resistance

We performed the experimental analysis of the ME-PEH under maximized average power conditions in different operational modes, which required different external loads R_{ML}. Here R_{ML} values were determined by calculating P_{av} as a function of R_L (figure 9(a)) for each plucking regime of interest:

$$P_{av} = \frac{V_{rms}^2}{R_L} = \frac{1}{R_L}\left(\sqrt{\frac{1}{k}\left(\sum_{i=1}^{k} V^2(t_i)\right)}\right)^2, \quad (1)$$

where $V(t_i)$ – instantaneous voltage values, k – the number of recorded voltage values, RMS voltage calculated as follows:

$$V_{\text{rms}} = V_{\text{rms}}(t_k) = \sqrt{\frac{1}{k}\left(\sum_{i=1}^{k} V_{\text{ML}}^2(t_i)\right)}, \tag{2}$$

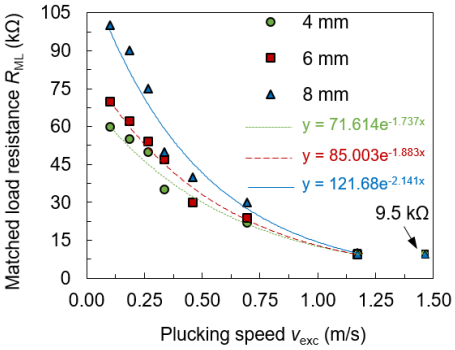

Figure 7. Measured matched load resistance versus v_{exc} for different d_{exc} including the exponential best-fit lines.

here $V_{\text{ML}}(t_i)$ – instantaneous voltage values ($R_{\text{L}} = R_{\text{ML}}$), k – the number of analyzed V_{ML} values, Δt – sampling interval. We observe in figure 7 that faster plucking ($v_{\text{exc}} \geq 1.17$ m/s) corresponds to values of R_{ML} which settle to ~9.5 kΩ. Also, it is visible that R_{ML} diminishes with increasing v_{exc} and decreasing d_{exc}. It is related to the decrease of magnetic force ramping times $t_{\text{R}}(F_y)$ and $t_{\text{R}}(F_x)$ in comparison with the rise time of the transducer $t_{\text{R}}(\text{PT})$, where higher plucking speed induces free vibrations of the transducer which oscillates at a natural frequency $f_{\text{n}} = 80$ Hz. It corresponds to the R_{ML} value of 9.5 kΩ (figure 7), which is close to the theoretical value of $R_{\text{opt}} = 1/2\pi f_{\text{n}} C_{\text{PT}} = 9.95$ kΩ determining the load resistance that is optimally matched to the capacitance-dominated impedance of the piezoelectric transducer excited at its resonant frequency.

3.3 ME-PEH oscillatory phases and operational modes

This experimental study presents an analysis of dynamic and electric characteristics of ME-PEH operational cycles that are achieved under varying magnetic plucking regimes. An operational cycle may be referred as a *total dynamic response (TDR)* of the transducer after it has been affected by a discrete transient excitation event, which in this chapter corresponds to a single magnetic pluck (figure 8). RMS voltage and average power calculated by formulas (1–2) and total cumulative energy that are generated up to a given instance of time t_k is calculated as:

$$E = E(t_k) = \sum_{i=1}^{k} \frac{V_{\text{ML}}^2(t_i)}{R_{\text{ML}}} \Delta t, \tag{3}$$

where $V_{ML}(t_i)$ – instantaneous voltage values (R_L = R_{ML}), k – the number of analyzed V_{ML} values, Δt – sampling interval. In other words, total energy E is the time integral of instantaneous power and it quantifies how much electrical energy is extracted from the ME-PEH during different oscillatory phases. The complete

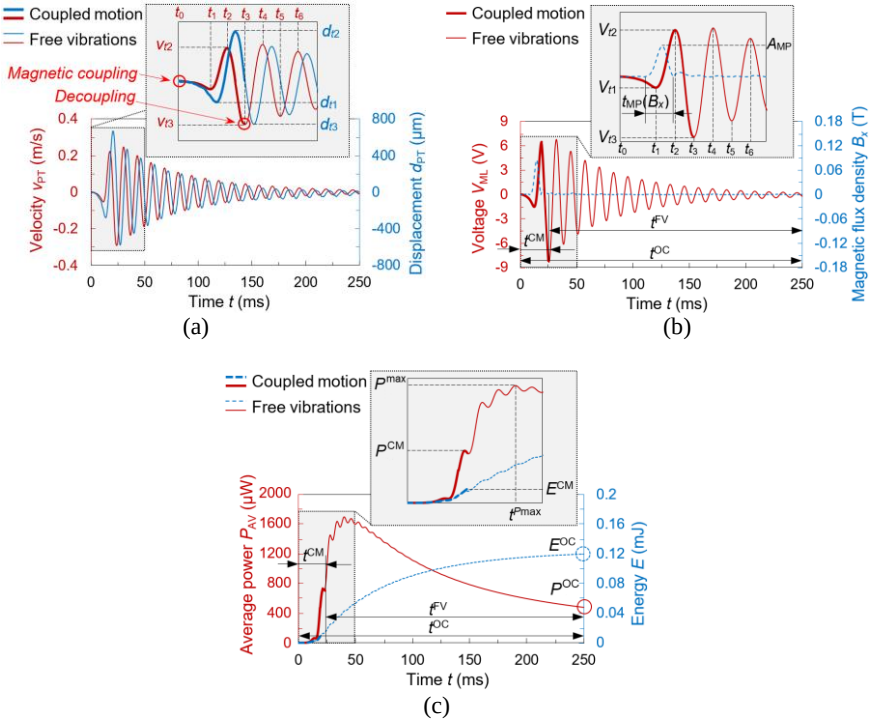

Figure 8. Representative transient velocity and displacement responses generated by the ME-PEH (d_{exc} = 6 mm) operating in (a) dynamic mode (v_{exc} = 1.44 m/s) and measured (b) transient voltage and magnetic field intensity responses and (c) the corresponding variation of average power and total commutative energy (generated by the ME-PEH operating in thedynamic mode at v_{exc} = 1.44 m/s, d_{exc} = 6 mm).

operational cycle is examined, then t_k = t^{OC} and the calculated electric characteristics are expressed as P^{OC} and E^{OC} (figure 8(c)). t^{OC} = 250 ms was used for the calculation since during this time interval the responses undergo a near-complete decay, which matches to a settling level of the response that meets the criterion of ±2% (which is usually applied for second-order dynamic systems subjected to impulsive excitation).

The whole operational performance of the ME-PEH may be subdivided into three *operational modes: dynamic*, *quasi-static* and *transitory*. The dynamic mode is achieved when a relatively high plucking speed v_{exc} induces the impulsive excitation of the transducer (figure 8). In the dynamic mode the transducer-forced vibration response, referred hereto as the *coupled motion (CM)* phase, is progressed into the *free vibration (FV)* phase with clean exponentially decaying free oscillations at natural frequency f_n. Here the transient characteristics of the CM phase determine the initial conditions for the subsequent FV phase. Relatively low v_{exc} leads to the least effective quasi-static mode of the ME-PEH since the transducer suffers magnetically-constrained deflection, where the very gradually deactivating magnetic coupling slowly releases the transducer. An intermediate plucking regime is induced when v_{exc} is higher than in the quasi-static mode but still not high enough to produce true impulsive excitation.

3.4 Analysis of the ME-PEH operation

The operational characteristics of the ME-PEH are determined by a complex relationship between the conditions of magnetic coupling and dynamic characteristics of the transducer (e.g. natural frequency f_n, damping ratio ζ_m). These conditions are governed by various interrelated factors, such as magnetic plucking regime (v_{exc} and d_{exc}), dimensions, shape and material properties of the interacting magnets, considering their arrangement in terms of polarization directions, alignment and spatial layout. The operation of the ME-PEH is analyzed in detail by varying the plucking regime, while the other conditions are left constant. Measurement results in Figure 9 present that the E^{OC} and P^{OC} values in the quasi-static and transitory modes are at least 15 and 3 times lower (Figures 9(a–b), respectively, in comparison with the peak output at $v_{exc} = 1.44$ m/s ($t_{MP}(B_x)$ / $T_n \cong 0.6$). Hence, these two modes should be avoided and a MFU-based energy harvester should be designed to perform in the highly effective dynamic mode. It is important to determine the threshold plucking conditions that allow to terminate the intermedia mode and induce the dynamic one. We take into consideration the general threshold criterion that classifies mechanical excitation as impulsive one (i.e. shock) when the ramping time of the affecting force is less than half the first natural period of a structure, i.e. $t_R(F_x) / T_n \lesssim 0.5$ in the case of a bell-shaped excitation impulse. Simulation results of force component F_y (Figure 5(b)) determine the highly effective plucking regime at $1.44 < v_{exc} < 1.84$ m/s, which corresponds to $0.36 < t_{jump} / T_n < 0.46$ or $0.73 < t_R(F_y) / t_R(PT) < 0.93$. Here $t_{jump} / T_n \cong 0.46$ or $t_R(F_y)/ t_R(PT) \cong 0.93$ presents the absolute peak of electrical output. Thus, we may conclude the key criteria for highly effective plucking: vibration energy harvesting performs at maximized operating regime when the dominant deflection force duration t_{jump} and the corresponding ramping time $t_R(F_y) = 0.5t_{jump}$ are marginally smaller than the natural half-period and rise time of the transducer,

respectively. Overly high plucking speeds (beyond ~1.84 m/s) cause excessively small force ramping times with respect to the rise time of the transducer, which leads to lower response amplitudes and decreased energy harvesting performance (i.e. descend region in Figure 9).

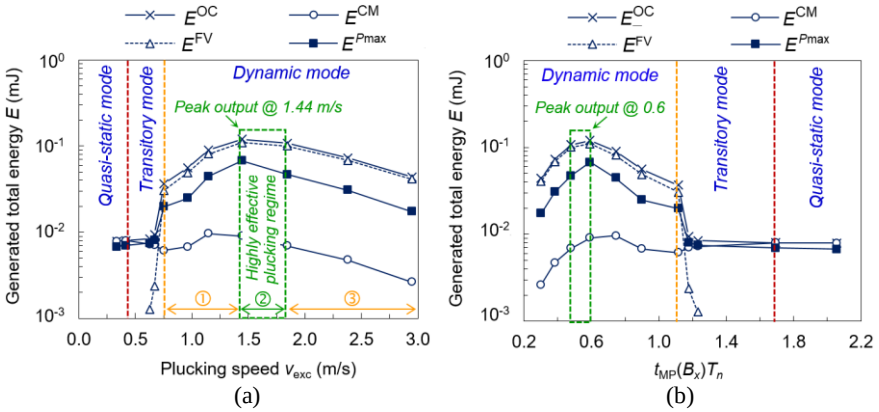

Figure 9. Semi-log plot of measured total cumulative energy (generated during time intervals t^{OC}, t^{CM}, t^{FV} and t^{Pmax}) versus (a) plucking speed and (b) dimensionless B_x impulse duration (d_{exc} = 6 mm). Regions of the dynamic mode: ① ascend, ② peak/plateau and ③ descend.

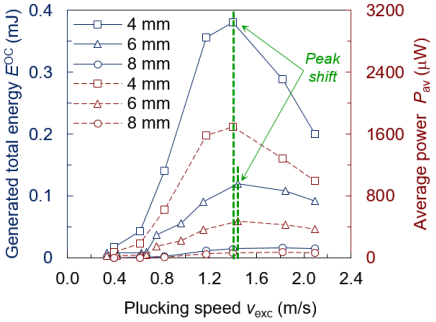

Figure 10. Total energy and average power generated during complete operational cycle t^{OC} versus plucking speed for different clearances d_{exc}.

Smaller clearances lead to stronger magnetic forces (Figure 3), which correspond to larger deflections of the transducer and higher electrical outputs. For example, peak output magnitudes tripled when d_{exc} reduced from 6 mm to 4 mm (Figure 10). Even more, clearance d_{exc} modifies the shape of the peak/plateau region, i.e. smaller d_{exc} leads to a peakier region, which represents higher sensitivity to variation in v_{exc}. At larger d_{exc}, maximum electrical outputs may be reached over a wider v_{exc} range. Meanwhile smaller clearances d_{exc} shift the peak point slightly to the left, which implies that a lower plucking speed is necessary to generate peak power outputs. It may be explained by faster force

ramping at smaller d_{exc}, which is obvious from the reduction in $t_{MP}(F_x)$ and t_{jump} (Figure 5).

4. A NOVEL BODY-MOUNTED PIEZOELECTRIC ENERGY HARVESTER BASED ON SYNCHRONIZED MULTI-MAGNET EXCITATION

4.1 Proof-of-concept of multi-magnet-excited piezoelectric energy harvester

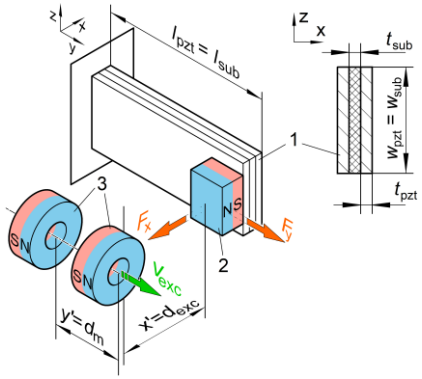

Figure 11. Schematics of a magnetically plucked piezotransducer: 1 – piezoceramic bimorph transducer, 2 – magnetic end mass (driven magnet) and 3 – driving magnet, l_{pzt}, w_{pzt} and l_{sub}, w_{sub} – length and width of the transducer piezoceramic and passive layers, respectively, t_{pzt} – thickness of piezoceramic layers, t_{sub} – thickness of a passive layer (substrate), v_{exc} – excitation (plucking) speed, d_{exc} – gap between driven and driving magnets, d_m – gap between driving magnets.

dimensions of R15×r6×6 mm transverse nearby the transducer magnetic end mass (driven magnet with dimension of 5×5×3 mm). Clearance d_{exc} is the distance between the driving and driven magnets along the *y*-axis when their positions are congruent

This chapter designs the ME-PEH to employ an out-of-plane plucking configuration, thereby involving a mechanical frequency up-conversion in the device (Figure 11). The device is based on a commercially-available transducer (Piezo Systems T226-A4-503Y) with dimensions of 57.2×31.8 mm. This type of transducer was chosen due its high strain (charge) constants, permittivity and high voltage output that are promising for sensing and generating devices. The transducer starts to vibrate at high-frequency free vibrations f_n when ring-shaped driving magnets with the

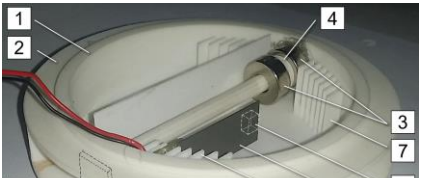

Figure 12. Proof-of-concept of multi-magnet P-VEH and its testing by attaching on upper limb of a person jogging on a treadmill (1 – housing, 2 – inertial rotor, 3 – a pair of driving magnets, 4 – insert for regulating d_m, 5 – outline of the driven magnet (invisible), 6 – piezoelectric transducer (bimorph), 7 – slots for regulating d_{exc}, 8 – amplification magnet with its outline, 9 – slots for inserting inertial mass).

along the *x*-axis (Figure 1). From a mechanical point of view, the magnetically induced deflection forces are treated as dynamic, and transient analysis is performed to predict electrical outputs. Here the motion of the driving magnets is induced by the amplification magnet, since it moves due to external human body excitation. The ME-PEH consist of an inertial rotor with eccentric mass and several amplification magnets with the dimensions of 10×10×2 mm which are attached around the rotor (Figure 12). Amplification and driving magnets are arranged so that they operate at the repelling regime (magnets' north poles turned to each other). Clearance between the amplification magnet and the driving magnet d_a allows to adjust the magnetic pushing force and the constant driving magnet(s) velocity as well. Smaller d_a causes higher and almost constant excitation speed v_{exc}. This allows to employ several multi-magnet excitation configurations, where a couple of plucking actions correspond to a nearly sinusoidal excitation shape. Further in this work we analyze traditional single-magnet and proposed multi-magnet excitation cases. However, this method may be developed using a larger amount of magnets.

The dimensions of the driving and amplification magnets were chosen with consideration to their strength, which is necessary to ensure a high driving magnet speed. Herewith, the dimensions and strength of magnets determine the overall device height and diameter, respectively. In order to exploit the entire area of the device, the maximum dimension transducer was realized inside. Briefly, the proposed ME-PEH includes these functions i) electric power generation in the transducer due direct piezoefect; ii) driving magnet(s) velocity amplification; iii) *synchronically muti-magnet excitation* (SME).

4.2 A numerical study of multi-excitation

M-PEH 2D model was developed with COMSOL Multiphysics® software. *Solid Mechanics* and *Piezoelectric Effect* modules were used to characterize a horizontally clamped cantilevered transducer (PZT-5A with the dimensions of 28.6×17.7 mm) with two piezo ceramic layers on exterior surfaces and one ground electrode at the middle. In order to receive a higher voltage output V_{ML} individual piezo ceramic layers were connected to an external resistor $R_{ML} = 10$ kΩ in parallel through *Electrical Circuit* interface. Since dynamic analysis is made in the effective plucking regime (transducer excited to vibrate at the first natural frequency).

In the model (Figure 13), the driving and amplification magnets were located above the transducer, while the driven one was modelled (attached) on the left transducer end. Magnetic coupling evaluation required to place all elements (including transducer magnetic end mass) into an air domain with a dimensions of 40×60 mm, which also set the normal component of the magnetic flux density to

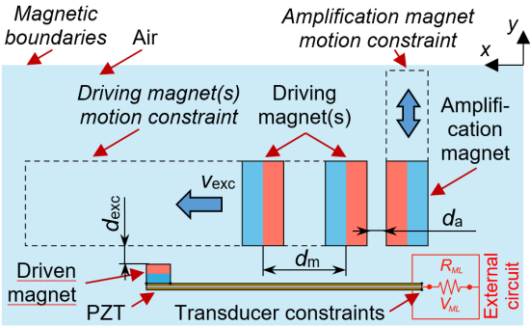

Figure 13. Schematics of the implemented finite element model of the P-VEH based on multi-magnet out-of-plane plucking, which also exploits amplification of plucking speed v_{exc} for power output increase when subjected to time-varying ultralow frequency body movements.

zero at the domain boundaries ($\mathbf{n} \cdot \mathbf{B} = 0$) in *Magnetic Fields, No Currents* interface. The size of the air domain was defined by taking into account the spread of magnetic field around the magnets and the analyzed range of driving and amplification magnets' displacements. A dynamic analysis of the driving magnet and its deflected transducer was implemented by using the *Mathematics* module with *Moving Mesh* (ALE) interface because a complete analysis needed dynamic mesh updating while solving for magnetic forces in the air domain. The driving magnet velocity provided by the amplification magnet was computed from magnetostatic analyzes with external analytical calculations. Parametric magnetostatic analysis between amplification and driving magnets was made in order to calculate forces at any magnet position, where the amplification magnet moves in $y(M_A)$ and driving one in $x(M_D)$ directions. Finally, the dynamic parameters of the driving magnet could be analytically calculated according $a(s(t), y(M_A), x(M_D)) = F_{amp} / m$; $v(t) = v_0 + at$; $s(t) = s_0 + v_0 t + 1/2at^2$, where t – elapsed time, F_{amp} – magnetic pushing force, m – driving magnet mass, a – driving magnet acceleration at time, s_0 and v_0 – initial displacement from the origin and initial velocity, $s(t)$ and $v(t)$ – displacement from the origin and velocity at time t. This simplification was done in order to reduce high computational costs in the magnetodynamic model, especially where the range of amplification magnet motion is considerably larger in comparison to the size of air domain elements.

4.3 Analysis of multi-magnet plucked of piezoelectric energy harvester

In this paper, the excitation of the P-VEH is implemented as an out-of-plane plucking of the bimorph. The experimental study was performed to estimate the most effective plucking speed considering clearance d_{exc} = 6 mm, which collectively influence the process of mechanical frequency up-conversion and the resulting vibration energy harvesting performance. The experimental study of magnetic plucking was performed measuring electric transient responses with an

oscilloscope PICO 6403. Transient voltage responses V_{ML} and the corresponding average power output (Figure 2(b)) were recorded with a transducer connected to the matched load resistor R_{ML} = 10 kΩ.

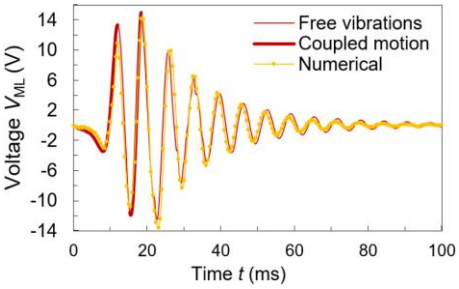

Figure 14. Experimental and numerical transient voltage responses V_{ML} generated by ME-PEH operating at the most effective plucking regime (d_{exc} = 6 mm, v_{exc} = 3 m/s).

During out of-plane plucking, when two driving magnets traverse past the driven one, two impulsive excitations deflect the transducer several times so that they can induce higher generated voltage (Figure 14). Experimental and numerical results show well agreement with about 5% mismatch of generated voltage signals, which leads to the conclusion that the developed numerical model is suitable for ME-PEH analysis in a transient dynamic regime. Depending on the distance between driving magnets d_m, magnetic couplings can be continuous or they can be activated with separation. This could be describe as two magnetic coupling and decoupling moments. For example, Figure 15(a) presents a highly effective multi-plucking regime when magnetic coupling of the second driving magnet appears at the same moment as the first magnet decoupling i.e. between d_{t2} and d_{t3} (v_{exc} = 3 m/s, d_{exc} = 6 mm). It is not graphically indicated but the moments of coupling and decoupling could not match to each other, which suggests that ME-PEH operates at a non-effective plucking regime.

In order to achieve a highly effective plucking regime we analytically estimated the distance d_a = 1.5 mm, which predetermined to v_{exc} = 2.99 m/s. Further numerical study proved that at this plucking speed single and multi ME-PEH reached the highest displacement amplitudes, which confirms that the generator operates in a highly effective plucking regime when dominant deflection force rising time $t_{ramp}(F_y)$ is close to transducer rising time t_{rise}. I.e. $t_{ramp}(F_y)/\ t_{rise} \cong$ 0.92 – 1.2 at $v_{exc} \cong$ 2.8 – 3.1 m/s. Figure 8 shows that multi excitation maximum average power output P^{OC} is 33% higher than a single excitation. It should be highlighted that this advantage was achieved only during effective plucking regime. Average power outputs started to diminish at a higher rate of change when excitation speed shifts away from the effective plucking speed of $v_{exc} \cong$ 3 m/s (Figure 6(a)). If effective plucking speed is ensured (constant), the distance

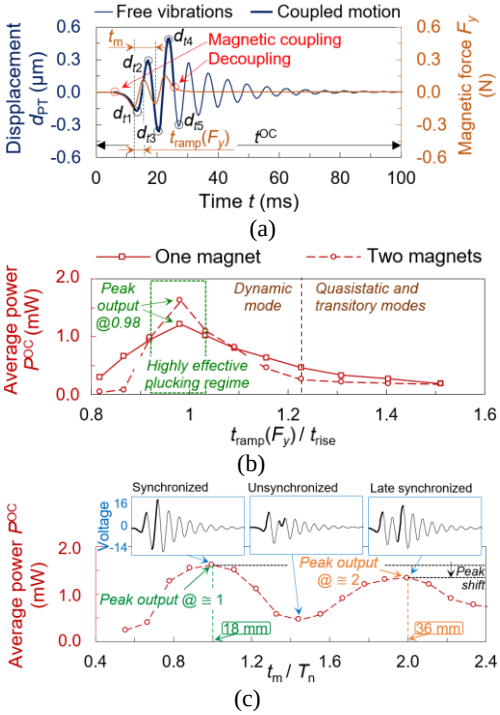

Figure 15. (a) Simulated transient signals of displacement d_{PT} and magnetic force F_y when P-VEH operates in a multi-magnet excitation regime, (b) simulated average power of single- and multi-magnet P-VEH versus dimensionless ratio of impulse duration $t_{ramp}(F_y)$ (d_m = 18 mm), (c) simulated average power of multi-magnet harvester versus dimensionless time duration between repeated magnetic impulses and transducer natural period. d_{exc} = 6 mm, v_{exc} = 3 m/s.

between two driving magnets d_m could also determine the power output increment or reduction which can be named as three ME-PEH operating regimes: i) well synchronized, ii) unsynchronized, iii) late synchronized (Figure 15(c)). For example, the well synchronized regime was described by d_m = 18 mm which caused two impulsive excitations where the duration between magnetic coupling moments was close to transducer's natural period (t_m/T_n = 1). The unsynchronized regime caused power output reduction because the second driving magnet suppressed free oscillations of the first one. The late synchronized regime allowed to achieve more power than in the unsynchronized regime, but less than in the synchronized one. This regime could appear then t_m/T_n = 2, 3… Generally multi-magnetic plucking is a complex loading case since magnetic couplings act along different axes, produce dissimilar complex-shaped impulses which could cause positive transducer deflection and negative free vibration suppression. Even more, ME-PEH operates at the effective regime then plucking speed and time duration between pluckings are well matched (synchronized), i.e. since the d_m could be adjusted once during device fabrication, any deviation of v_{exc} could cause a drastic degradation of power output. This is the biggest challenge for biomechanical applications where the speed of human movements is not stable and changes in a wide range. The velocity amplification method allows to eliminate this issue and ensure a stable and constant plucking speed during any frequency of motion.

Summarizing the results, the ME-PEH operating at the SME regime generates 33% higher average power and total cumulative energy during t^{OC} = 100 ms (t/T_n = 14) comparing with the single plucking regime. Here P^{OC} reaches only ~32% of maximum possible power P^{max}, which is achieved at t/T_t = 4.4 (Figure 16). Meanwhile maximum possible power P^{max} in the single plucking regime is achieved at t/T_t = 4.4. This reveals that the SME regime prolongs higher amplitudes transient response zone from 2.4 < t/T_t < to 4.4 and a point located at t/T_n = ~5 could be defined as the moment of the most effective duration when the ME-PEH is characterized by the highest amount of average power with the lowest loss in total cumulative energy, i.e. ~90% of all available power and energy is harvested during the successive operational cycle.

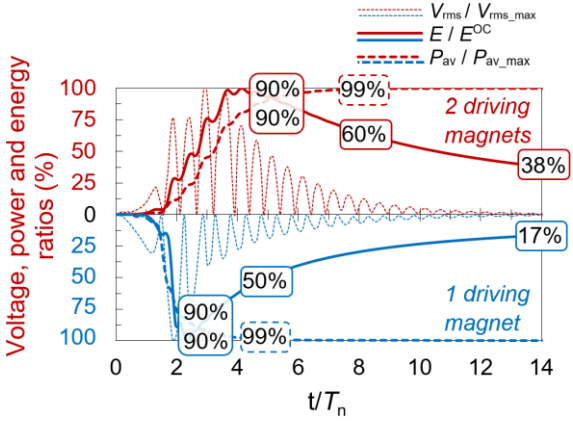

Figure 16. Average power and total energy ratios versus dimensionless time (d_{exc} = 6 mm, v_{exc} = 3 m/s).

4.4 Testing of multi-magnet P-VEH in real operating conditions

A proof-of-concept P-VEH was fabricated by using 3D printing facilities and manual assembly. The device was attached on the upper arm of a person who was jogging on a treadmill at different speeds (Figure 17(a)), thereby producing the expected actual operating conditions of the energy harvester. Figure 17(b) provides typical transient voltage signals together with the respective average power which were generated at treadmill speeds of 7 km/h and 11 km/h (P-VEH was connected to the matched load resistance). It may be observed that the treadmill speed has no appreciable influence on the amplitude of the voltage signals, which demonstrates operational stability. It means that the P-VEH operates in the most effective plucking regime (the transducer is impulsively excited at transient resonance) essentially regardless of the jogging speed. The observed ~15% difference between the voltage peaks that were recorded at

different treadmill speeds may be attributed to the random nature of biomechanical excitations. More specifically, it should be noted that the transducer (mounted inside the device housing) is not isolated from irregular inertial excitations, which act in addition to the intended excitation via magnetic plucking. Meanwhile, the higher average power observation delivered during faster jogging is caused by a higher number of complete operational cycles that fit into the recording time interval of 1000 ms (5 cycles correspond to P^{OC} = 0.48 mW at 7 km/h, meanwhile 6 cycles correspond to P^{OC} = 0.58 mW at 11 km/h).

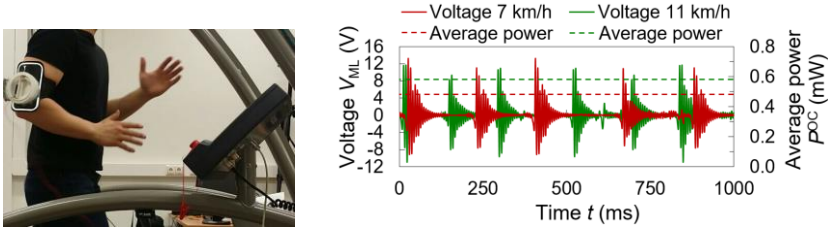

(a) (b)

Figure 17. (a) Proof-of-concept of multi-magnet P-VEH and its testing by attaching on an upper limb of a person jogging on a treadmill (b) Measured transient voltage responses and average power of the device tested at different treadmill speeds.

CONCLUSIONS

1. Biomechanical piezo-generators have a wide application potential in portable and wearable electronic devices. However, it is very difficult to generate high power output using low-frequency human movements because a piezo-generator produces usable electrical power levels only at higher vibration frequencies ($P \propto f^3$). Mechanical frequency up-conversion based on magnetic coupling (M-MFU) is a suitable approach to generate high-frequency free vibrations of the piezo-generator.
2. Developed numerical models allowed to identify the main static and dynamic characteristics of magnetic interaction. It was determined that the duration of force direction reversal t_{jump} and the respective force ramping time $t_{ramp} = 0.5t_{jump}$ are critical excitation parameters that govern the operational conditions of M-MFU.
3. A combined numerical-experimental study allowed to determine the most important dynamic principles that govern performance of the piezo-generators operating on the basis of M-MFU. Main results are as follows:

3.1 For generating usable power outputs it is necessary to induce dynamic mode (impulsive excitation) by achieving high speed of the driving magnet so that dimensionless excitation parameters satisfy the condition of $t_{jump} / T_n < 1$ ($t_{ramp} / t_{rise} < 2$). Electrical outputs are ~15 and ~3 times higher in the dynamic mode than in the quasi-static and transitory modes, respectively.

3.2 For generating maximized power output it is necessary to induce impulsive excitation that activates transient resonance, which is achieved when t_{jump} becomes marginally smaller than the natural half-period of the transducer, i.e. $t_{jump} / T_n \cong 0.45 - 0.5$ ($t_{ramp} / t_{rise} \cong 0.9 - 1.0$). During transient resonance the response amplitudes are maximized and frequencies of the forced and free vibration responses become equal to the natural frequency f_n, which is very useful because it is sufficient to apply a constant matched load resistance.

3.3 The established main principles of magnetic coupling dynamics and the identified values of dimensionless excitation parameters may be directly applied to rationally designing various magnetically-excited transducers of arbitrary natural frequency and magnetic configuration.

4. The magneto-piezo-mechanical FE model of the designed proof-of-concept piezo-generator does not require the application of computationally-intensive COMSOL Moving Mesh method (ALE) and allows to calculate dynamic and electric characteristics with less than ~10% error.
5. In comparison to the conventional single-magnet excited piezo-generator, the proposed synchronized multi-magnet excitation method enables an increase of the electrical outputs up to 33 % at transient resonance. The proposed method is only effective when the following conditions are satisfied: i) the distance between the magnets d_m is tailored to satisfy $t_m \cong T_n$ and ii) the piezo-generator is impulsively excited by achieving $t_{jump} / T_n < 1$.
6. The proof-of-concept piezo-generator was fabricated and tested on the treadmill under the targeted operating conditions. It was determined that the proposed methods of magnet speed amplification and synchronized multi-magnet excitation generator are effective in delivering a relatively stable impulsive excitation of the transducer under biomechanical excitations of different frequency (the variability of the generated voltage amplitudes does not exceed ~15%).

LITERATURE

1. DAUKŠEVIČIUS R., BRIAND D. Energy harvesting // Material-integrated intelligent systems: technology and applications / edited by Stefan Bosse, Dirk Lehmhus, Walter Lang, and Matthias Busse. Weinheim: Wiley-VCH, 2018. ISBN 9783527336067. eISBN9783527679249. pp. 479-528. doi: 10.1002/9783527679249.ch21.
2. Briand D., Yeatman E., Roundy S. Micro Energy Harvesting, First Edition. © Wiley-VCH Verlag GmbH & Co. KGaA. 2015 byWiley-VCH Verlag GmbH & Co. KGaA. doi: 10.1109/UPEC.2016.8114023.
3. PRIYA S., INMAN JD. Energy Harvesting Technologies. New York: Springer. 2009, 9-34. doi: 10.1007/978-981-10-3815-0_2.
4. XUE T., ROUNDY S. On magnetic plucking configurations for frequency up-converting mechanical energy harvesters. Sensors Actuators A-Phys. 253. 2017, 101-11. doi: 10.1016/j.sna.2016.11.030.
5. WEI C., JING X. A comprehensive review on vibration energy harvesting: Modelling and realization. Renewable Sustainable Energy Rev. 74. 2017, 1-18. doi: 10.1016/j.rser.2017.01.073.

LIST OF PUBLICATIONS RELEVANT TO DISSERTATION
ARTICLES IN PEER-REVIEWED SCIENTIFIC PUBLICATIONS

Indexed in the Web of Science with Impact Factor

International Publishers

1. Dauksevicius, Rolanas; Kleiva, Arunas; Grigaliunas, Valdas. Analysis of magnetic plucking dynamics in a frequency up-converting piezoelectric energy harvester // Smart materials and structures. Bristol : IOP Publishing. ISSN 0964-1726. eISSN 1361-665X. 2018, vol. 27, iss. 8, art. no. 085016, p. 1-19. DOI: 10.1088/1361-665X/aac8ad. [Scopus; Science Citation Index Expanded (Web of Science)] [IF: 2,963; AIF: 3,588; IF/AIF: 0,825; quartile: Q1 (2017, InCites JCR SCIE)] [CiteScore: 3,38, SNIP: 1,474, SJR: 1,152 (2017, Scopus Sources)] [M.kr.: T 009] [Input: 0,334].

National Publishers

2. Kleiva, Arūnas.; Daukševičius, Rolanas. Experimental study of multi-magnet excitation for enhancing micro-power generation in piezoelectric vibration

energy // Mechanika / Kaunas University of Technology, Vilnius Gediminas Technical University, Lithuanian Academy of Sciences. Kaunas : KTU. ISSN xxxx-xxxx. 2019, T. xx, nr. x, p. 1-6. DOI: xxxx. [M.kr.: T 009] [Input: 0,50]. *In print.*

Articles in conference proceedings

International Publishers

3. Kleiva, Arūnas; Daukševičius, Rolanas. Numerical and experimental study of a novel body-mounted piezoelectric energy harvester based on synchronized multi-magnet excitation // EuroSimE 2019: proceedings of the 20th International Conference on Thermal, Mechanical and Multi-Physics Simulation and Experiments in Microelectronics and Microsystems, 24, 27 March 2019, Leibniz University of Hannover, Germany / ISSN xxxx-xxxx. 2019, p. 1-6. DOI: xxxx. [M.kr.: T 009] [Input: 0,50]. *In print*

National Publishers

4. Kleiva, Arūnas; Daukševičius, Rolanas. Experimental study of dynamic and electric characteristics of piezoelectric transducer excited by magnetic forces // Mechanika 2016 : proceedings of the 21st international scientific conference, 12, 13 May 2016, Kaunas University of Technology, Lithuania / Kaunas University of Technology, Lithuanian Academy of Science, IFTOMM National Committee of Lithuania, Baltic Association of Mechanical Engineering. Kaunas : Kauno technologijos universitetas. ISSN 1822-2951. 2016, p. 144-148. [Conference Proceedings Citation Index - Science (Web of Science)] [M.kr.: T 009] [Input: 0,500].
5. Kleiva, Arūnas; Daukševičius, Rolanas. Experimental study of footstrike-induced impulse excitation for biomechanical energy harvesting // Mechanika 2015 : proceedings of the 20th international scientific conference, 23, 24 April 2015, Kaunas University of Technology, Lithuania / Kaunas University of Technology, Lithuanian Academy of Science, IFTOMM National Committee of Lithuania, Baltic Association of Mechanical Engineering. Kaunas : Kauno technologijos universitetas. ISSN 1822-2951. 2015, p. 155-159. [Conference Proceedings Citation Index - Science (Web of Science)] [M.kr.: T 009] [Input: 0,500].

INFORMATION ABOUT AUTHOR

Arūnas Kleiva was born in 1989 in Gudžiūnai, Kėdainių d.
2008-2012: Studies in Kaunas University of Technology, Faculty of Mechanics and Mechatronics, Bachelor's degree in Mechatronic Engineering.
2012-2014: Studies in Kaunas University of Technology, Mechanical Engineering and Design, Master's degree in Manufacturing Engineering.
2004-2018: Doctoral studies in Kaunas University of Technology, Faculty of Mechanical Engineering and Design, (Technological Sciences, Mechanical Engineering (T 009)).
E-mail: arunas.kleiva@gmail.com

REZIUMĖ

Temos aktualumas

Nuolatos gausėjantys mokslo tiriamieji darbai energijos surinkimo/generavimo tematikoje rodo, kad autonominių savikrovių (angl. „self-powered“) elektroninių įrenginių poreikis nepaliaujamai didėja. Absoliuti dauguma įvairios paskirties nešiojamų, dėvimų bei implantuojamų išmaniųjų sistemų veikia naudodamos tradicines baterijas ar akumuliatorius, kurie funkcionalumo, komfortabilumo ir ekologiškumo atžvilgiu vis labiau nebetenkina dabartinės visuomenės poreikių. Elektrocheminiai energijos šaltiniai vartotojams asocijuojasi su nuolatiniais baterijų keitimo ar akumuliatorių įkrovimo rūpesčiais. Taip pat, akivaizdu kad tvaraus vartojimo kontekste būtinybė tinkamai utilizuoti elektrocheminių elementų kenksmingas atliekas yra rimta aplinkosauginė problema. Mus supančioje aplinkoje ypač gausu kinetinės energijos įskaitant ir biomechaninę energiją žmogaus kūno dalių judesių pavidalu. Todėl vienais iš perspektyviausių yra laikomi vibraciniai energijos generatoriai su įterptomis sumaniosiomis pjezo medžiagomis. Dėl nesudėtingos konstrukcijos (sąlyginai nesudėtingas miniatiūrizavimas) ir pakankamai aukšto pjezo medžiagų energetinio tankio pjezoelektriniai vibraciniai energijos generatoriai yra neretai pranašesni mikro/meso lygmenyje už analogiškus elektromagnetinius, elektrostatinius ar triboelektrinius įrenginius. Tam kad energijos generatorius veikdamas ultra-žemo dažnio biomechaninio sužadinimo metu generuotų didesnį kiekį elektros energijos naudojamas *mechaninis dažnio aukštinimo* (MDA) (angl. „mechanical frequency up-conversion“) metodas. kuris yra vienas perspektyviausių pjezogeneratorių veikimo efektyvinimo metodų žemadažnėje aplinkoje.

Tyrimo tikslas ir uždaviniai

Tyrimo tikslas – suprojektuoti, pagaminti ir ištirti biomechatroninių sistemų pjezoelektrinį vibracinį energijos generatorių, praktiškai panaudojamą žemadažnio biomechaninio sužadinimo sąlygomis.

1. Atlikti egzistuojančių biomechaninių vibracinių energijos generatorių literatūros apžvalgą, didžiausią dėmesį skiriant dažnio aukštinimo principu veikiančių pjezogeneratorių konstrukcijų ypatumams.
2. Sudaryti dažnio aukštinimo procese dalyvaujančios magnetinės sąveikos skaitinius modelius, atlikti jų analitinį ir eksperimentinį verifikavimą bei analizę, siekiant įvertinti sužadinimo impulsų dinamines charakteristikas.
3. Taikant skaitinius ir eksperimentinius tyrimo metodus, ištirti magnetinio sankybio pagrindu funkcionuojantį vibracinio energijos generavimo procesą, siekiant nustatyti esminius dinamikos principus ir kiekybinius kriterijus, būtinus projektuojant praktiškai panaudojamus biomechaninius pjezogeneratorius.
4. Sudaryti ir verifikuoti projektuojamo biomechaninio pjezogeneratoriaus skaitinį dinaminį modelį ir atlikti skaičiavimus, siekiant įvertinti įrenginio vibracines ir elektrines charakteristikas.
5. Realizuoti ir ištirti magnetinio sužadinimo (dažnio aukštinimo) proceso efektyvinimo būdus, siekiant padidinti biomechaninio pjezogeneratoriaus pagaminamos elektros energijos kiekį sudėtingomis žemadažnio sužadinimo sąlygomis.
6. Suprojektuoti, pagaminti ir ištestuoti realiomis sąlygomis dėvimą pjezoelektrinį energijos generatorių, kuriame pritaikyti pasiūlyti efektyvinimo metodai.

Mokslinis naujumas

1. Atskleisti magnetinio sankybio pagrindu veikiančių pjezogeneratorių esminiai dinamikos dėsningumai ir, pritaikius bedimensinius kintamuosius parametrus, nustatyti ribinio ir veiksmingiausio magnetinio sužadinimo kiekybiniai kriterijai, kuriuos tenkinant pasiekiama santykinai aukšta arba didžiausia elektrinė galia.
2. Sudaryti mažiau skaičiavimo resursų reikalaujantys magnetodinaminės bei magneto-pjezo-mechaninės sąveikos baigtinių elementų modeliai, kuriuos taikant kartu su identifikuotais kiekybiniais dinaminiais kriterijais, galima racionaliai projektuoti įvairios magnetinės konfigūracijos ir tikrinio dažnio magnetinio sankybio pagrindu veikiančius pjezogeneratorius, veikiančius didžiausios galios režimu.
3. Magnetinio sankybio pagrindu veikiančių pjezogeneratorių veikimui efektyvinti pasiūlyti magnetinio įgreitinimo ir sinchronizuoto

daugiamagnetinio sužadinimo metodai, kurie užtikrina pakankamai tylų ir patikimą įrenginio veikimą didžiausios galios režimu (pareinamojo rezonanso aplinkoje) plačiame biomechaninio žadinimo parametrų intervale.

Ginamieji teiginiai

1. Pasitelkus kombinuotos skaitinės-eksperimentinės tyrimų metodiką įrodyta, kad maksimalus elektros energijos kiekis pagaminamas tada, kai keitiklis veikia pereinamojo rezonanso režimu, kai susilygina virpesių dažnis visuose pereinamojo atsako etapuose (priverstinių ir laisvųjų virpesių fazėse).
2. Daugiafizikinis magneto-pjezo-mechaninis baigtinių elementų modelis sudaro galimybes nedideliais kompiuteriniais resursais pakankamai tiksliai prognozuoti įvairios sudėtingos magnetinės konfigūracijos, dažnio aukštinimo principu veikiančių pjezogeneratorių dinamines ir elektrines charakteristikas.
3. Magnetinio įgreitinimo metodas yra saugus (patvarus) ir veiksmingas bekontaktinio mechaninio sužadinimo būdas, užtikrinantis nagrinėjamo pjezogeneratoriaus veikimą didžiausios galios režimu (pareinamojo rezonanso aplinkoje), kai įrenginys yra žadinamas aktyviai judančio žmogaus rankų mostais.
4. Sinchronizuoto daugiamagnetinio sužadinimo metodas yra veiksmingas ir sudaro galimybes naudojant du varančiuosius magnetus trečdaliu padidinti generuojamos energijos kiekį kiekvieno įrenginio veikimo ciklo metu (palyginti su atveju, kai sužadinimui pasitelkiamas vienas magnetas).
5. Sukurtas dėvimas biomechaninis pjezogeneratorius yra originalios konstrukcijos, į kurią racionaliai integruotos magnetinio įgreitinimo ir sinchronizuoto daugiamagnetinio sužadinimo posistemės (netrukdo viena kitai tinkamai funkcionuoti), užtikrinančios pakankamai tylų įrenginio darbą didžiausios galios režimu įvairiomis biomechaninio sužadinimo sąlygomis.

Praktinė vertė

1. Baigtinių elementų modeliai ir identifikuoti kiekybiniai dinaminiai kriterijai yra naudingi kuriant įvairių konstrukcinių parametrų pjezogeneratorius, veikiančius magnetinio sankybio pagrindu.
2. Daugiakanalis nekontaktinių matavimų stendas, sinchroniškai registruojantis dinaminius ir elektrinius / magnetinius sistemos parametrus, gali būti naudojamas įvairios magnetinės konfigūracijos pjezogeneratorių eksperimentiniams tyrimams.
3. Magnetinio įgreitinimo ir sinchronizuoto daugiamagnetinio sužadinimo metodai gali būti pritaikomi efektyvinti magnetinį sužadinimą įvairiuose pjezogeneratoriuose, veikiančiuose magnetinio sankybio pagrindu.

4. Pasiūlytoji biomechaninio pjezogeneratoriaus konstrukcija gali būti miniatiūrizuota ir pritaikyta įkrauti akumuliatoriams įvairiuose nešiojamuose / dėvimuose elektronikos įrenginiuose (fiziologinės būklės stebėsenos prietaisuose, išmaniuosiuose įrenginiuose ir kt.).

Pirmame, literatūros apžvalgos, skyriuje pateikta bendroji mikroenergijos generatorių analizė, apžvelgti įvairūs biomechaninių generatorių tipai ir veikimo principai, aptarti jų trūkumai ir pranašumai.

Antrame skyriuje aptartas tiriamo pjezogeneratoriaus, veikiančio magnetinio sankybio (mechaninio dažnio aukštinimo) pagrindu, veikimo principas. Aprašyti sudaryti magnetostatinis ir magnetodinaminis baigtinių elementų modeliai, skirti analizuoti sąveiką tarp dviejų nuolatinių magnetų, atliktas modelių verifikavimas ir skaičiavimai, kuriais nustatomos svarbiausios sistemoje veikiančių magnetinių jėgų ypatybės, įvertintos sužadinimo impulsų laikinės ir amplitudinės charakteristikos.

Trečiame skyriuje pateikiamas atliktas išsamus magnetinio sankybio pagrindu veikiančio vibracinio energijos generavimo proceso tyrimas. Pritaikius eksperimentinius ir skaitinius metodus, sistemingai išnagrinėti pjezogeneratoriaus veikimo režimai įvairiomis magnetinio sužadinimo sąlygomis. Išanalizavus nekontaktinių matavimų stende išmatuotus pereinamuosius atsakus, nustatytos magnetinių jėgų deformuojamo keitiklio dinaminių ir elektrinių charakteristikų priklausomybės nuo sužadinimo parametrų. Apibūdinti svarbiausi pjezogeneratoriaus dinamikos ir energijos generavimo dėsningumai, identifikuotos ribinio ir efektyviausio sužadinimo sąlygos.

Ketvirtame skyriuje pateikiami pjezogeneratoriaus magnetinio sužadinimo efektyvinimo metodai: magnetinis įgreitinimas ir sinchronizuotas daugiamagnetinis sužadinimas. Aprašytas sudarytas daugiafizikinis magneto-pjezo-mechaninis baigtinių elementų modelis, atliktas eksperimentinis jo verifikavimas. Pateiktas pagal matematinius modelius suprojektuotas ir pagamintas dėvimo biomechaninio pjezogeneratoriaus maketas su integruotomis sužadinimo efektyvinimo posistemėmis. Pateikti maketo laboratorinių bandymų rezultatai, gauti imitavus realias įrenginio eksploatavimo sąlygas, išnagrinėtos išmatuotos dinaminės ir elektrinės charakteristikos.

Disertacijos išvadose apibendrinami svarbiausi atliktų teorinių ir eksperimentinių tyrimų rezultatai.

Išvados

1. Išsami egzistuojančių biomechaninių energijos generatorių literatūros apžvalga atskleidė, kad vibraciniai pjezogeneratoriai dėl aukšto energijos tankio ir miniatiūrizavimo galimybių turi plačias perspektyvas būti panaudoti šiuolaikiniuose autonominiuose dėvimuose ar nešiojamuose elektroniniuose

įrenginiuose. Veikimo efektyvumo prasme esminis pjezogeneratorių trūkumas yra tas, kad juose didesni elektros energijos kiekiai yra gaminami tik rezonanso aplinkoje aukštesnių dažnių intervale. Tačiau, biomechaniniai pjezogeneratoriai yra žadinami itin žemo dažnio žmogaus kūno judesiais (< 10 Hz), o tai reiškia, kad įrenginio elektrinė galia yra labai nedidelė ($P \propto f^3$). Šiame darbe išnagrinėtas magnetinis dažnio aukštinimo metodas yra vienas perspektyviausių pjezogeneratorių veikimo efektyvinimo žemadažnėje aplinkoje būdų.

2. Sudarytais matematiniais modeliais įvertintos svarbiausios statinės ir dinaminės magnetinės sąveikos charakteristikos. Nustatyta, kad magnetinės jėgos reversijos trukmė t_{rev}, o kartu ir jėgos užaugimo trukmė $t_{UT} = 0.5t_{rev}$ yra pagrindiniai sužadinimo parametrai, kurie nusako nagrinėjamo dažnio aukštinimo proceso funkcionavimo sąlygas.
3. Gauti eksperimentiniai ir skaitiniai rezultatai leido atskleisti svarbiausius energijos generavimą lemiančius dinamikos dėsningumus:
   3.1 Siekiant realizuoti pjezogeneratoriaus veikimą dinaminiame (impulsinio sužadinimo) režime, būtina naudoti aukštą varančiojo magneto greitį, kuris užtikrintų tai, kad bedimensiniai magnetinio sužadinimo parametrai tenkintų sąlygą $t_{rev} / T_t < 1$ ($t_{UT} / t_K < 2$). Nustatyta, kad dinaminiame režime generuojama vidutinė galia ir suminė energija yra iki ~15 ir ~3 kartų didesnė nei, atitinkamai, kvazistatiniame ir pereinamajame režimuose.
   3.2 Veiksmingiausias impulsinio magnetinio sužadinimo režimas pasiekiamas keitikliui veikiant pereinamajame rezonanse, kurio metu generuojama didžiausia elektrinė galia. Pereinamasis rezonansas pasiekiamas tada, kai t_{rev} yra šiek tiek trumpesnė už keitiklio tikrinį pusperiodį, t. y. $t_{rev}/ T_t \cong 0.45 – 0.5$ ($t_{UT} / t_K \cong 0.9 – 1.0$). Rezonanso metu keitiklio virpesių dažnis priverstinių ir laisvųjų virpesių fazėse tampa lygus keitiklio pirmosios skersinių virpesių formos dažniui f_t, o tai rodo, kad elektrinė galia gali būti maksimizuojama naudojant vienodo dydžio suderintą varžą.
   3.3 Atskleisti efektyvų energijos generavimą lemiantys magnetinio sužadinimo principai ir bedimensinėje formoje pateikti kiekybiniai sužadinimo kriterijai pritaikomi projektuojant įvairios magnetinės konfigūracijos ir skirtingo tikrinio dažnio pjezogeneratorius, kurie veikia magnetinio sankybio (mechaninio dažnio aukštinimo) pagrindu.
4. Realizuotas pjezogeneratoriaus maketo skaitinis BE modelis (nenaudojantis didelių skaičiavimo resursų reikalaujančio judančio tinklelio metodo) leido nustatyti magnetinių jėgų deformuojamo keitiklio dinaminių ir elektrinių charakteristikų priklausomybes nuo sužadinimo parametrų su mažesne nei ~10 % paklaida.

5. Pjezogeneratorius, veikdamas pereinamajame rezonanse ir išnaudodamas įgreitinto SDS metodą, pasiekia apie 33 % didesnę vidutinę galią ir suminę energiją suderintos varžos sąlygomis nei įrenginys sužadinimui naudojantis vieną varomąjį magnetą. Siekiant, kad SDS metodas būtų veiksmingas, būtina naudoti aukštą ir pastovų sužadinimo greitį ir tinkamą nuo jo priklausomą atstumą tarp varančiųjų magnetų d_m. Šis greitis užtikrina impulsinį sužadinimą tuomet, kai keitiklio lenkime dominuojančios ašinės jėgos reversijos ir skersinės jėgos impulso bedimensinės trukmės (atitinkamai, t_{rev} / T_t ir $t(F_y)_{MI}$ / T_t) tampa mažesnės už vienetą. Kartu abu parametrai lemia trukmę tarp pakartotinų sužadinimų $t_m = d_m / v_{žad}$, kuri turi būti artima keitiklio tikriniam periodui ($t_m / T_t = \sim 1$).
6. Atlikus pagaminto pjezogeneratoriaus maketo veikimo bandymus ant bėgimo takelio, imituojant realias eksploatacines sąlygas, nustatyta, kad pasiūlyti varančiųjų magnetų įgreitinimo ir SDS metodai yra veiksmingi nes užtikrina pakankamai pastovų impulsinį keitiklio magnetinį sužadinimą esant kintamo dažnio biomechaninio žadinimo sąlygoms (generuojamų įtampos signalų amplitudžių sklaida neviršija ~15 %).

Darbo rezultatų aprobavimas

Disertacijoje pateikti tyrimų rezultatai buvo paskelbti penkiose publikacijose: dviejuose Web of Science duomenų bazėje referuojamuose leidiniuose su citavimo indeksu ir trijose publikacijose konferencijų pranešimų medžiagoje.

Tyrimų rezultatai pateikti trijose tarptautinėse konferencijose: EuroSimE 2019 (Hanoveris, Vokietija), Mechanika 2015, 2016 (Kaunas, Lietuva).

UDK 621.311.6-868 (043.3)

SL344. 2019-04-23, 2,25 leidyb. apsk. l. Tiražas 50 egz.
Išleido Kauno technologijos universitetas, K. Donelaičio g. 73, 44249 Kaunas
Spausdino leidyklos „Technologija“ spaustuvė, Studentų g. 54, 51424 Kaunas